Polymer Chemistry

Accepted Manuscript

ROYAL SOCIETY OF CHEMISTRY

www.rsc.org/polymers

Polymer Chemistry RSCPublishing

ARTICLE

Aromatic amine-sulfone/sulfoxide conjugated D–π–A–π–D type dyes in photopolymerization under 405nm and 455nm laser beams

Cite this: DOI: 10.1039/x0xx00000x

Received 00th January 2012,
Accepted 00th January 2012

DOI: 10.1039/x0xx00000x

www.rsc.org/

Mengqiang Wang,[a,b] Xiaoyu Ma, [b] Jinghua Yu,[b] Xiaoqin Jia, [b] Dandan Han, [b] Tengfei Zhou, [b] Jinliang Yang ,[b] Jun Nie[b] and Tao Wang[*a,b]

Based on a D–π–A–π–D structural strategy, six novel dyes (Cz-SO, Cz-SO_2, TA-SO, TA-SO_2, PTZ-SO, and PTZ-SO_2) containing triphenylamine/phenothiazine/carbazole as electron donors and sulfone/sulfoide as electron acceptors are prepared and incorporated into a photoinitiating system, together with iodonium salt (ONI). The one- and two-photon photophysical properties of these dyes were studied. The UV-vis spectra showed red-shifts of 51 and 75 nm from N-ethyl carbazole (CZ) to Cz-SO and Cz-SO_2. Similar red-shifts were found in the other dyes. The two-photon excited fluorescence (TPEF) spectra in the range 700-880 nm were measured and it was found that these dyes present a clear two-photon absorption (TPA). Among them, PTZ-SO2 possesses the maximum TPA cross-section which is 2465.5 GM. Ring-opening cationic polymerization of epoxides and free radical polymerization of acrylates upon exposure to very soft irradiation of laser diodes at 405 nm and 455 nm were performed using ONI/dyes initiating systems. Compared with the well-known camphorquinone-based systems, the combinations of the obtained dyes with iodonium salt exhibit higher polymerization efficiency. The results from photobleaching and electrochemical experiments show that these dyes could photosensitize ONI through photoinduced charge transfers. Owing to their higher polymerization efficiency and large TPA cross-section, these dyes would have extensive application prospects in the flields of photopolymerization by soft visible light irradiation sources and two-photon polymerization (TPP).

1 Introduction

Photoinitiated polymerization is a well-known technique used in many technologically important areas.[1-3] The recent development of cheap and easily accessible light-emitting diodes (LEDs) operating on soft visible light irradiations has opened new fields for photoinitiated polymerization. Compared with UV irradiation sources, soft visible light irradiation sources are more convenient and avoid UV rays. For polymer synthesis at soft irradiation conditions, the design and development of excellent photoiniators in the visible light wavelength range is a very challenging task.[4] However, exploring new photoinitiators used for radical photopolymerization, especially for cationic photopolymerization at soft irradiation conditions, is difficult.

Dye photosensitized photopolymerization reactions have been largely known for many years and typically encountered in various photopolymerizations. The design and synthesis of new chemical skeletons used as photosensitizers are easier than those of new photoinitiators. Recently, real progress has been made in the synthesis of new chemical skeletons and in the use of new additives, which has allowed the proposal of a large number of novel photoinitiating systems.[5-8] Several commercial dyes can be used in visible light induced photopolymerization, such as camphorquinone and anthraquinone derivatives. Chemically modified conventional UV sensitive photoinitiators were also found to be efficient visible light photosensitizers, such as chemically modified benzophenone derivatives,[9-11] chemically modified thioxanthone derivatives,[12] and chemically modified 2,2'-dimethoxy-2-phenylacetophenone derivatives. [13] Newly developed dyes applicable in visible light sensitive photoinitiating systems include purple or blue light sensitive dyes, green light sensitive dyes, red light sensitive dyes, and so on.[5.,6,14]

In cationic photopolymerization systems, onium salts, especially diaryliodonium salts, are widely used as photoinitiators because of their simple synthesis, absence of color, and high photoinitiating efficiency. However, the absorption of these salts generally occurs below 350 nm, which limits their applications under visible light. Several electron-rich polynuclear aromatic compounds, such as anthracene, pyrene, and perylene, have been reported to increase the spectral sensitivities of diaryliodonium salts in visible light and are especially attractive and efficient photosensitizers. Crivello and coworkers reported several carbazole and phenothiazine compounds bearing cationically polymerizable vinyl, vinyl ether, and epoxide groups.[15-20] These monomers are rapidly and efficiently polymerized or copolymerized by UV irradiation in the presence of onium salt photoinitiators.Several mechanisms explain the photosensitization of onium salts; however, the most efficient and generally applicable process for this class of photoinitiators is electron-transfer photosensitization. In these photosensitizing systems, diaryliodonium salt shows good electron-accepting ability with dyes.

Materials exhibiting large TPA are currently of great interest because of their applications in various fields such as multiphoton fluorescence microscopy, three-dimensional (3D) optical data storage, optical power limiting, and microfabrication.[21-25] To fully exploit the great potential of the TPA process, search for new compound exhibiting large TPA cross-section values is still one of the hot topics in those fields. General design strategies are to develop molecules with large changes of dipole/quadrupole moments upon excitation, with extended conjugation, etc. This can be achieved through structure motifs such as D-π-A, D-π-D, D-π-A-π-D, and A-π-D-π-A.

A great number of highly efficient two-photon absorbing systems were employed for two-photon initiated photopolymerization. For example, Nazir and coworkers synthesized a set of thioxanthone derivatives bearing strongly electrondonating dialkylamino groups witch all had two photon absorption;[26] Wu and coworkers synthesized particular novel benzylidene cyclopentanone dyes with a triphenylamine core with well sensitizing efficiency in two-photon photopolymerization;[27-29] Jin and coworkers synthesized a series of multibranched triphenylamine-based chromophores incorporating 4-(methylthio)styryl fragments as external substituents, which showed two photon absorption and good sensitization effect.[30]

In the present paper, to increase absorption in a visible light region, dyes based on a bipolar skeleton involving aromatic amine moiety linked to diphenyl sulfone/diphenyl sulfoxide through the bridge of acetylene were synthesized. These dyes all have the D-π-A-π-D character in the molecular structure. They were used as electron-transfer photosensitizers, and ring-opening cationic polymerization of epoxides and free radical polymerization of acrylates upon exposure to very soft irradiation of laser diodes at 405 nm and 455 nm were investigated. To expand the application of these aromatic amine-sulfone/sulfoxide conjugated D–π–A–π–D type dyes, their two-photon fluorescence properties were also studied and the TPA cross-sections were obtained.

2 Experimental details

2.1 Materials and instrument

N-Methylpyrrolidone (NMP), epichlorohydrin (ECH), and triethanolamine (TEA) were purchased from Beijing Chemical Works (Beijing, China). Camphorquinon (CQ) was obtained from Aldrich. Iodonium bis(4-methylphenyl)hexafluorophosphate (ONI) was used as a reference iodonium salt. Epoxy resin E51 (from Jiangsu Sanmu Company China) and tripropylene glycol diacrylate (TPGDA, from Etemal Chemical Co. Ltd. Zhuhai, China) were selected as representative oligomer and monomer. Di(4-bromophenyl) sulfoxide and di(4-bromophenyl) sulfone were prepared according to the reference procedure.[31,32] They were characterized by comparing their ^1H NMR spectra with that of one reported in references. Other chemicals used were of analytical reagent grade and used without further purification. Chromatographic purification of products was accomplished using 200-400 mesh chromatography silica. Thin-layer chromatography (TLC) was performed on 0.20 mm silica gel plates. Scheme 1 summarizes the abbreviations and structures of some compounds employed in this study.

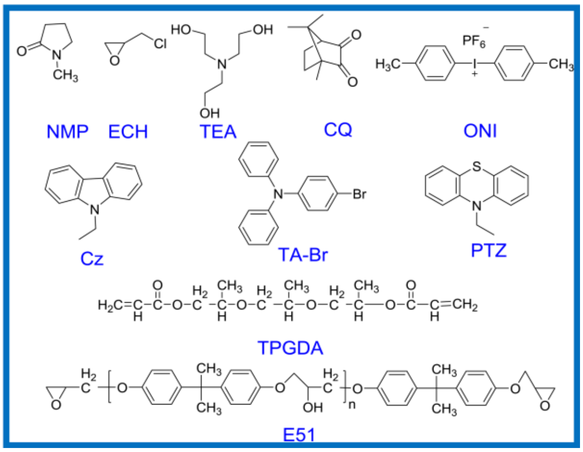

Scheme 1. Abbreviations and structures of NMP,ECH,TEA,CQ,ONI,Cz,TA-Br,PTZ,TPGDA and E51 .

^1H NMR and ^{13}C NMR spectra were determined by a Bruker AV400 (400 MHz) NMR spectrometer. The mass spectra (MS) were obtained on Nermag France (R10-10C) spectrometer. Elemental analysis was obtained by Vario EL cube (Elementar Analysensy steme Germany). IR spectroscopy was performed on Nicolet Avatar 370 MCT using KBr pellets. The electrochemical behavior of the bimolecular photoinitiator system was investigated by cyclic voltammetry with an LK3200A electrochemical workstation (Lanlike Chemistry and Electron High Technology Corporation, Tianjin, China). The irradiation sources were laser diodes at 405 nm (FU405GX200-BD2285, 100 mW) and 455 nm (FU455GX200-BD2285, 100 mW). The melting points of the compounds were determined using an XT-4 microscopic melting point apparatus. UV-vis absorption spectra were recorded on a UV-5200 (UNICO) UV-vis spectrophotometer. One-photon excited

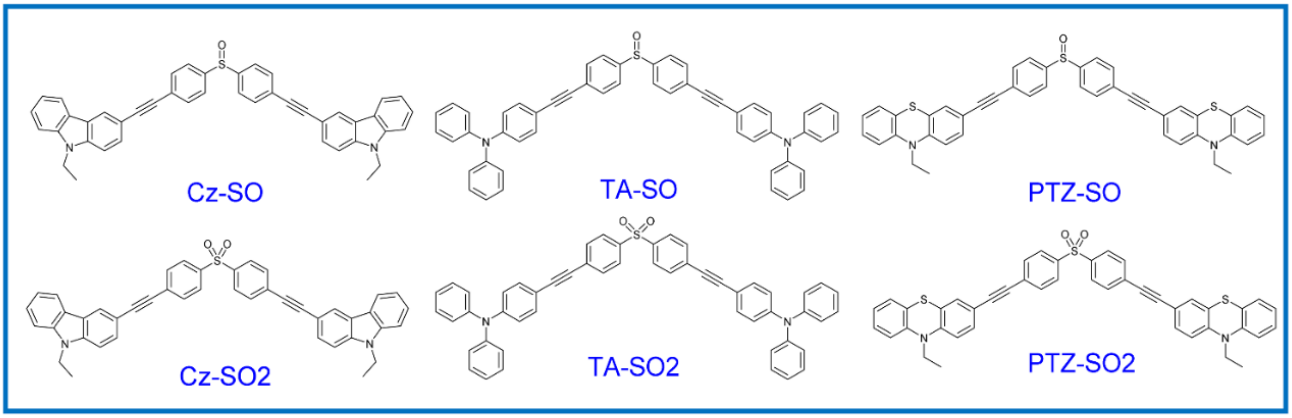

Scheme 2. The structure of the Cz-SO,Cz-SO2,TA-SO,TA-SO2,PTZ-SO and PTZ-SO2.

fluorescence spectra were recorded on an F-4500 (Hitachi High-Technologies Corporation) fluorescence spectrophotometer. Two-photon excited fluorescence (TPEF) spectra were recorded on SD2000 spectrometer (Ocean Optical) with excitation with a femtosecond laser (Tsunami, Spectra-Physics).

For all calculation, Gaussian 09 has been employed. The molecular structures in the ground state were optimized based on density function theory (DFT) at the Becke 3-Lee-Yang-Parr (B3LYP)/Genecp (C, H, N, and O with 6-31G** basis set).

2.2 Synthesis

2.2.1 Synthesis of ethynyl aromatic amine

Typically, $Pd(PPh_3)_2Cl_2$(0.3 mmol), CuI (8.0 mmol), PPh_3 (12.0 mmol) and bromine substituted aromatic amine (40.6 mmol) were dissolved in a solution of DMF (300 mL) and TEA(50 mL). The mixture was nitrogen bubbled for 30 min and then slow heated at 85 ℃. 2-Methyl-3-butyn-2-ol (61.0 mmol) was added to the reaction mixture and heated at 85 ℃ for 3.5 h under nitrogen. Thin-layer chromatography was used for monitoring the reaction. The result mixture was filtered to remove salts. The filtrate was concentrated and poured into the saturated NH_4Cl solution and then extracted with CH_2Cl_2. The organic phase was dried and using rotary evaporator to remove the solvent to obtain the intermediate alkynolyl aromatic amine.

The alkynolyl aromatic amine (29.7 mmol) was dissolved in 250 mL of isopropanol, to which pulverized KOH (86.2 mmol) was added. The mixture was refluxed under nitrogen with stirring for about 3 h. After that the mixture was poured into 300 mL water, the product was extracted with ethyl acetate, dried over anhydrous $MgSO_4$, then the solvent was evaporated. The crude product was purified by column chromatography (silica gel, pure petroleum ether) to give the product ethynyl aromatic amine. The scheme for synthesis of ethynyl aromatic amine was shown in Scheme. S1.

N-(4-ethynylphenyl)-N-phenylbenzenamine: A yellow solid (4.9 g, 61%). Mp: 113-114 ℃. δ_H (400 MHz, $CDCl_3$)[33]: 7.36 (2 H, d, J = 8.8 Hz), 7.30 (4 H, t, J = 7.2 Hz), 7.13 (4 H, d, J = 7.6 Hz), 7.09 (2 H, t, J = 7.4 Hz), 6.99 (2 H, d, J = 8.8 Hz), 3.05 (1 H, s). δ_C (101 MHz, $CDCl_3$) 148.4, 147.1, 133.1, 129.4, 125.1, 123.7, 122.1, 114.8, 83.9, 76.2.

N-ethyl-4-ethynylcarbazole: A yellow solid (3.6 g, 56%). Mp: 123-124 ℃. δ_H (400 MHz, $CDCl_3$)[34]: 8.29 (1 H, s), 8.12 (1 H, d, J = 8.0 Hz), 7.62 (1 H, d, J = 8.4 Hz), 7.52 (1 H, t, J = 8.0 Hz), 7.44 (1 H, d, J = 8.4 Hz), 7.37 (1 H, d, J = 8.4 Hz), 7.28 (1H, t, J = 8.4 Hz), 4.39 (2 H, q, J = 7.2 Hz), 3.09(1 H, s), 1.46 (3 H, t, J = 7.2 Hz). δ_C (101 MHz, $CDCl_3$) 140.2, 130.3, 130.2, 128.9, 124.9, 124.8, 123.4, 122.4, 112.7, 110.2, 108.7, 84.7, 75.5, 37.8, 13.8.

N-ethyl-4-ethynylphenothiazine: A yellow solid (4.7 g, 63%). Mp: 80-81°C. δ_H (400 MHz, $CDCl_3$): 7.31 – 7.27 (1 H, m), 7.25 (1 H, d, J = 2.4 Hz), 7.17 (1 H, t, J = 8.4 Hz), 7.12 (1 H, d, J = 7.6 Hz), 6.94 (1 H, t, J = 7.6 Hz), 6.88 (1 H, d, J = 8.4 Hz), 6.79 (1 H, d, J = 8.4 Hz), 3.94 (2 H, q, J = 7.2 Hz), 3.06 (1 H, s), 1.44 (3 H, t, J = 7.2Hz); δ_C (101 MHz, $CDCl_3$): 145.5, 144.2, 131.3, 130.6, 127.4, 127.4, 124.3, 123.7, 122.7, 115.7, 115.2, 114.6, 83.1, 76.8, 41.9, 12.9.

2.2.2 Synthesis of the six dyes

The structures of the dyes are shown in Scheme 2.

Typically, $Pd(PPh_3)_2Cl_2$ (0.1 mmol), CuI (0.5 mmol), PPh_3 (0.5 mmol) and di(4-bromophenyl) sulfoxide or di(4-bromophenyl) sulfone (5.0 mmol) were dissolved in a solution of DMF (150 mL) and TEA (30 mL). The mixture was nitrogen bubbled for 30 min and then slow heated at 85 ℃. Ethynyl aromatic amine (11.0 mmol) was added to the reaction mixture and heated at 85 ℃ for 3.5 h under nitrogen. Thin-layer chromatography was used for monitoring the reaction. The result mixture was filtered to remove salts. The filtrate was concentrated and poured into the saturated NH_4Cl solution and then extracted with CH_2Cl_2. The organic phase was dried and using rotary evaporator to remove the solvent to obtain the crude product. The product was purified on a silica gel column using PE/DCM as the eluent and the pure products were obtained. The scheme for synthesis of Cz-SO, Cz-SO_2, PTZ-SO and PTZ-SO_2 were shown in scheme 3 and the scheme for synthesis of TA-SO and TA-SO2 were shown in Scheme. S2.

TA-SO

A yellow solid (2.4 g, 65%). Mp: 164-165 ℃. δ_H (400 MHz, $CDCl_3$): 7.62 (4 H, t, J = 8.8 Hz), 7.61 (4 H, t, J = 8.4 Hz), 7.38(4 H,

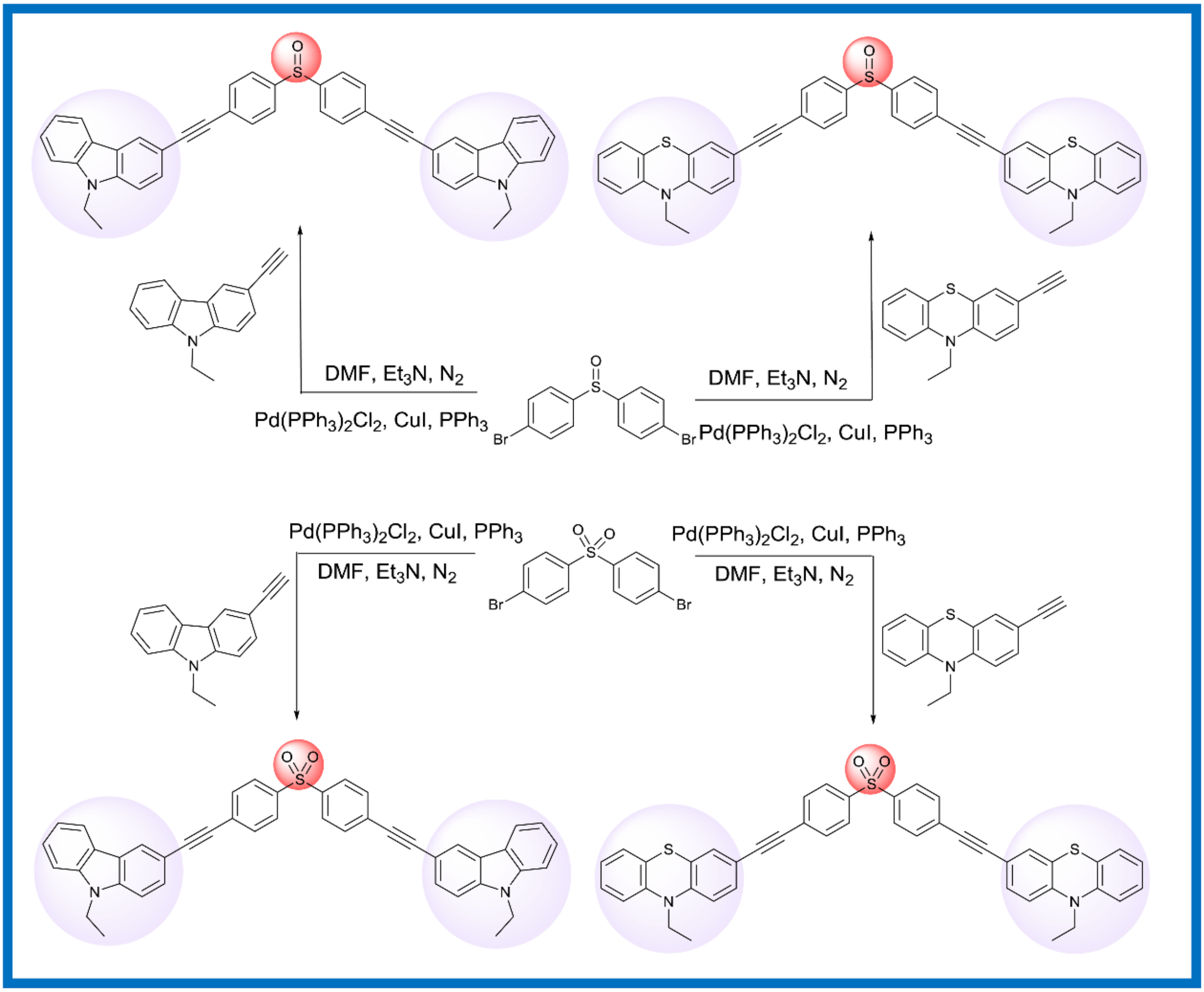

Scheme 3.The scheme for synthesis of Cz-SO, Cz-SO$_2$, PTZ-SO and PTZ-SO$_2$.

d, J = 8.8 Hz), 7.31 (8 H, t, J = 7.6 Hz), 7.14 (8 H, d, J = 8.4 Hz), 7.10 (4 H, t, J = 7.2 Hz), 7.02 (4 H, d, J = 8.8 Hz); δ C (101 MHz, CDCl3):148.4, 147.1, 144.5, 132.7, 132.1, 129.1, 126.9, 125.2, 124.8, 123.8, 121.9, 115.1, 92.4, 87.5; IR (KBr, ν/cm^{-1}): 3037 (Ar-H), 2210.5 (C≡C), 1585, 1508 and 1490 (C=C), 1278.3 (C-N), 1044.9 (SO); MS m/z: 737 (M$^+$). Elemental analysis calc. for $C_{52}H_{36}N_2OS$: C, 84.75; H, 4.92; N, 3.80; S, 4.35%; found: C, 84.83; H, 4.92; N, 3.81; S, 4.33 %.

TA-SO2

A yellow solid (2.3g, 61%). Mp: 208-209 °C. δ_H (400 MHz, CDCl$_3$): 7.92 (4 H, d, J = 8.4 Hz), 7.62 (4 H, d, J = 8.4 Hz), 7.38(4 H, d, J = 8.4 Hz), 7.31 (8 H, t, J = 8.4 Hz), 7.14 (8 H, d, J = 7.6 Hz), 7.11 (4 H, t, J = 7.2 Hz), 7.02 (4 H, d, J = 8.4 Hz); δ_C (101 MHz, CDCl$_3$): 148.7, 146.9, 140.0, 132.8, 132.0, 129.5, 129.2, 127.6, 125.3, 123.9, 121.7, 114.6, 94.1, 87.2; IR (KBr, ν/cm^{-1}): 3037 (Ar-H), 2207 (C≡C), 1583, 1509 and 1490 (C=C), 1279 (C-N), 1235 (C-N), 1328 and 1164 (SO$_2$); MS m/z: 753 (M$^+$). Elemental analysis calc. for $C_{52}H_{36}N_2O2S$: C, 82.95; H, 4.82; N, 3.72; S, 4.26%; found: C, 83.02; H, 4.85; N, 3.71; S, 4.24 %.

PTZ-SO

A yellow solid (2.2 g, 63%). Mp: 101-102 ℃. δ_H (400 MHz, Acetone): 7.79 (4 H, d, J = 8.4 Hz), 7.68 (4 H, d, J = 8.4 Hz), 7.38 (2 H, d, J = 8.4 Hz), 7.28 (2 H, d, J = 2.0 Hz), 7.22 (2 H, t, J = 8.4 Hz), 7.14 (2 H, d, J = 7.6 Hz), 7.05 (4 H, t, J = 7.6 Hz), 6.98 (2 H, t, J = 7.6 Hz), 4.03 (4 H, q, J = 6.9 Hz), 1.40 (6 H, t, J = 6.8 Hz); δ_C (101 MHz, Acetone): 147.1 , 146.4, 145.7, 133.0, 132.0, 130.5, 128.6, 128.0, 127.1, 125.4, 125.2, 124.4, 123.8, 117.1, 116.6, 116.1, 95.1, 88.9 , 42.5, 13.1; IR (KBr, ν/cm^{-1}): 3056 (Ar-H), 2925 and 1395 (C-H), 2207 (C≡C), 1573, 1499 and 1463 (C=C), 1234 (C-N), 1084.8 (SO); MS m/z: 701 (M$^+$). Elemental analysis calc. for $C_{44}H_{32}N_2OS_3$: C, 75.40; H, 4.60; N, 4.00; S, 13.72%; found: C, 75.51; H, 4.61; N, 3.99; S, 13.69 %.

PTZ-SO2

A brown solid (2.3 g, 63%). Mp: 124-125 ℃. δ_H (400 MHz, Acetone): 8.03 (4 H, d, J = 8.4 Hz), 7.74 (4 H, d, J = 8.8 Hz), 7.40 (2 H, d, J = 8.4 Hz), 7.30 (2 H, d, J = 2.0 Hz), 7.21 (2 H, t, J = 8.4 Hz), 7.14 (2 H, d, J = 7.6 Hz), 7.06 (4 H, m), 6.98 (1 H, t, J = 7.6 Hz), 4.03 (4 H, q, J = 6.8 Hz), 1.40 (6 H, t, J = 6.8 Hz); δ_C (101 MHz, Acetone): 146.8, 144.9, 141.7, 133.0, 132.2, 130.6, 129.6, 128.8, 128.6, 128.0, 125.1, 123.9, 123.8, 116.6, 116.6, 116.1, 93.7, 88.6, 42.5, 13.1; IR (KBr, ν/cm^{-1}) : 3058 (Ar-H), 2928 and 1397 (C-H), 2208 (C≡C), 1588, 1500 and 1464 (C=C), 1325 and 1159 (SO_2); MS m/z: 717 (M^+). Elemental analysis Calc. for C44H32N2O2S3: C, 73.71; H, 4.50; N, 3.91; S, 13.42%; found: C, 75.83; H, 4.53; N, 3.89; S, 13.38 %.

Cz-SO

A light yellow solid (1.9 g, 59%). Mp: 188-189 ℃. δ_H (400 MHz, $CDCl_3$): 8.32 (2H, s), 8.12 (2 H , d, *J* = 7.6 Hz), 7.79 – 7.61 (10 H, m), 7.53 (2 H, t, *J* = 7.6 Hz), 7.45 (2 H, d, *J* = 8.4 Hz), 7.41 (2 H, d, *J* = 8.4 Hz), 7.33 – 7.25 (2 H, m), 4.40(4 H, q, *J* = 7.2 Hz), 1.48 (6 H, t, *J* = 7.2 Hz); δ_C (101 MHz, $CDCl_3$): δ 144.5, 140.4, 139.7, 132.2, 129.4, 127.4, 126.3, 124.9, 124.4, 122.9, 122.5, 120.6, 119.5, 112.5, 108.8, 108.6, 93.1, 86.4, 37.7,13.8; IR (KBr, ν/cm^{-1}): 3049 (Ar-H), 2974 and 1382 (C-H), 2208 (C≡C), 1626, 1585, 1493 and 1474 (C=C), 1229 (C-N), 1087 (SO); MS m/z: 637 (M^+). Elemental analysis calc. for $C_{44}H_{32}N_2OS$: C, 82.99; H, 5.07; N, 4.40; S, 5.03%; found: C, 83.11; H, 5.10; N, 4.39; S, 4.98 %.

Cz-SO2

A yellow solid (2.2 g, 66%). Mp: 251-252 ℃. δ_H (400 MHz, $CDCl_3$): 8.33 (2H, s), 8.13 (2 H, d, *J* = 8.0 Hz), 7.96 (4 H, d, *J* = 8.4 Hz), 7.70 (4 H, d, *J* = 8.4 Hz), 7.66 (2 H, d, *J* = 8.4 Hz), 7.54 (2 H, t, *J* = 6.8 Hz), 7.46 (2 H, d, *J* = 8.0 Hz), 7.42 (2 H, d, *J* = 8.8 Hz), 7.30 (2 H, t, *J* = 7.2 Hz), 4.40 (4 H, q, *J* = 7.2 Hz), 1.48 (6 H, t, *J* = 7.2 Hz); δ_C (101 MHz, $CDCl_3$): δ 140.4, 140.0, 139.8, 132.0, 129.6, 129.4, 127.7, 126.3, 124.5, 123.1, 122.5, 120.6, 119.6, 112.1, 108.8, 108.6, 95.4, 86.3, 37.8, 13.8; IR (KBr, ν/cm^{-1}): 3054 (Ar-H), 2974 and 1383 (C-H), 2209(C≡C), 1627, 1587, 1495 and 1475 (C=C), 1231 (C-N), 1321 and 1156 (SO_2); MS m/z: 653 (M^+). Elemental analysis calc. for $C_{44}H_{32}N_2O_2S$: C, 80.96; H, 4.94; N, 4.29; S, 4.91%. found: C, 81.01; H, 4.95; N, 4.28; S, 4.90 %.

2.3 NIR spectroscopy measurement

IR spectra were recorded on a Nicolet 5700 instrument (Thermo Electron Corporation, Waltham, MA). Near infrared (NIR) spectroscopy was used to measure the double bond and epoxy group conversion as a function of exposure time in the resins. All samples were photocured in 1.8 mm thick plastic molds with a 10 mm diameter center. The molds were clamped between two glass slides. The samples were irradiated with monochromatic light delivered by laser diodes at 405nm or laser diodes at 455nm. The distance is 15cm between irradiation light and sample, the light intensity were 2 mW/cm^{-2} and 30 mW/cm^{-2}, respectively. For each sample, the NIR runs were repeated three times. The specimens were irradiated at different time intervals by manually controlling the curing light. Upon collection of the uncured resin NIR spectrum, spectra were obtained immediately after each exposure interval. The double bond conversion profiles were calculated from the decay of the absorption band located at 6,165 cm^{-1} as described by Stansbury and Dickens.[35] The epoxy conversion was calculated from the decay of the absorption band located at 6,075 cm^{-1}.[36] The conversion was calculated using Eq. (1):

$$\text{Conversion \%} = [1-S_t/S_0] \times 100\% \qquad \text{Eq. (1)}$$

where S_t is the area of the absorbance peak when the irradiating period is t. S_0 is the initial area of the absorbance peak.

2.4 Electrochemical experiments

Cyclic voltammetric measurements were performed on a LK3200A electrochemical workstation, using 1.0 mM dye solution in DCM at a scan rate of 100 mV/s, using 0.1 M tetrabutyl ammonium hexafluorophosphate as supporting electrolyte, before experiments the solutions was nitrogen bubbled for 30 min. The glassy carbon, standard calomel electrode (SCE) and platinum were used as working, reference and auxiliary electrodes, respectively.

2.5 Free energy changes of photoinduced electron transfer

The free energy change ΔG_{et} is an important parameter for the electron transfer (ET) process. If ΔG_{et} is negative, the ET process is thermodynamically allowed.[37, 38] In this paper, the ΔG_{et} for the ET reaction between the excited state of an ONI as an electron acceptor and the dyes as the electron donor were calculated based on the Rehm−Weller equation (Eq. (2)),[38] in this paper $E_{ox}(D/D^{\bullet+})$ is the oxidation potential of the electron donor, $E_{red}(A^{\bullet-}/A)$ is the reduction potential of the electron accepter. E_{00} is the singlet excited state energy obtained by Eq. (3).[39] Where h is Planck constant, c is the speed of light. λ is the wavelength at intersection of the fluorescence excitation and emission spectra; $Ze^2/\varepsilon a$ is Coulombic energy and considered negligible with respect to the overall magnitude of ΔG_{et}. E_{ox} and E_{red} were obtained from the cyclic voltammetric curve.

$$\Delta G_{et} = E_{ox}\left[\frac{D}{D^{\cdot+}}\right] - E_{red}\left[\frac{A^{\cdot-}}{A}\right] - \frac{Ze^2}{\varepsilon a} - E_{00} \qquad \text{Ep. (2)}$$

$$E_{00}=hc/\lambda \qquad \text{Ep. (3)}$$

2.6 State photolysis experiment

The dyes with the presence of ONI in DCM were irradiated under the laser diodes at 455nm (I_0≈30 mW cm^{-2}). The irradiated systems were consisted of 1 mL ONI (1 mM) and different volume dyes (0.01 mM), the distance is 15cm between irradiation light and sample, the light intensity was 30 mW/cm^{-2}, and we must make sure m_{dye}:m_{ONI}=1:10. Then the UV-vis spectra were recorded on a UV-5200 (UNICO) UV-vis spectrophotometer at different irradiation times.

2.7 Fluorescence quantum yields experiment

OPEF spectra were recorded at the concentrations of 1.0 ×10^{-5} mol/L in DCM on an F-4500 fluorescence spectrophotometer. The fluorescence quantum yields were obtained with quinine sulfate dihydrate (1×10^{-6} mol/L) in 0.1 M sulfuric acid aqueous solution as a reference standard (Φ_{ref} =0.54) by Eq. (4), [40] and the dyes concentrations was 1.0 ×10^{-6} mol/L in DCM.

$$\Phi = \frac{A_{ref} n^2 F}{A n_{ref}^2 F_{ref}} \Phi_{ref} \quad \text{Eq. (4)}$$

where Φ is the quantum yield, n is the refractive index, *A* is the absorbance of solution at the exciting wavelength, and *F* is the integrated area under the emission spectrum.

2.8 Two-photon excited fluorescence experiment

TPEF spectra were recorded on SD2000 spectrometer with excitation with a femtosecond laser (Tsunami, Spectra-Physics). This laser provided pulses of 100-fs of duration at a repetition rate of 80 MHz and was tunable in the wavelength range of 700-880 nm. The laser beam was focused into a quartz cell of 1 cm path length by using a 5 cm focal-length lens. The excitation intensity was 8.2 GW/cm^2 and the laser spot diameter is 2 mm. To calculate the TPEF cross sections, Rhodamine B in methanol solution (1×10^{-4} mol/L) was utilized as references for the calculation. For the six dyes, a DCM solution (1×10^{-4} mol/L) was prepared to calculate the TPEF cross sections. All the samples and standards were tested under the same experimental conditions. The TPA cross section δ_{TPA} was then calculated by the Eq. (5)[41]:

$$\delta = \delta_{ref} \frac{\Phi_{ref} c_{ref} n_{ref} F}{\Phi c n F_{ref}} \quad \text{Eq. (5)}$$

where Φ was the fluorescence quantum yield of the sample as stated in equation (4). δ is the TPA cross-sectional value, c is the concentration of the solution, n is the refractive index of the solution, F is the TPEF integral intensities of the solution emitted at the exciting wavelength. The δ_{ref} value of reference was taken from the literature.[42]

3.Results and discussion

3.1 UV-vis absorption

The UV-vis absorption spectra of the dyes in dichlormethane (DCM) are shown in Fig 1. Fig 1 (a) was measured at the concentrate of 1×10^{-5} mol/L, whereas the spectra in Fig 1 (b) were measured at the concentrate of 1×10^{-3} mol/L. The results of the absorption measurements are summarized in Table 1. The results show that the intramolecular chargetransfer (ICT) absorption band of these dyes are located at 350-490 nm. Specifically, among these dyes, TA-SO2 and PTZ-SO2 show strong absorption at about 400 nm, making them suitable with the 405 nm laser beams. For comparison, the absorption spectra of N-ethyl carbazole (CZ), bromo triphenylamine (TA-Br), and N-ethyl phenothiazine (PTZ) were measured (shown in Fig. S1 and Fig. S4). The maximum absorption wavelength of the dyes has more red-shift than CZ, TA-Br, and PTZ. In detail, Cz-SO and Cz-SO2 are longer (51 and 75 nm) than CZ; TA-SO and TA-SO2 are longer (70 and 85 nm) than TA-Br; and PTZ-SO and PTZ-SO2 are longer (57 and 75 nm) than PTZ. The results also reveal that the maximum absorption of Cz-SO2 has a longer wavelength than that of Cz-SO. The same case can be found at the absorption spectra of other dyes. The reason is that the electron-withdrawing ability of sulfone is stronger than that of sulfoxide.

Table 1 Light absorption properties of the dyes

	λ_{max} (nm)	$\varepsilon\times10^5$ (M^{-1}cm^{-1}) (λ_{max})	$\varepsilon\times10^4$ (M^{-1}cm^{-1}) (405nm)	$\varepsilon\times10^3$ (M^{-1}cm^{-1}) (455nm)
Cz-SO	351	1.07	0.03	0.06
Cz-SO2	369	0.77	0.05	0.08
TA-SO	374	1.34	3.31	2.65
TA-SO2	389	1.16	8.95	5.07
PTZ-SO	370	0.56	3.08	1.58
PTZ-SO2	388	0.55	4.73	8.04
Cz	294	0.18	----	----
TA-Br	304	0.15	----	----
PTZ	313	0.03	----	----

In Table 1, the molar extinction coefficients (ε) of these dyes at 405 and 455 nm are given. The order of absorption strength of these dyes at 405 nm is TA-SO2>PTZ-SO2>TA-SO>PTZ-SO>Cz-SO2>Cz-SO, and the order of absorption strength at 455 nm is PTZ-SO2>TA-SO2>TA-SO>PTZ-SO>Cz-SO2>Cz-SO. The absorptions of Cz-SO2 and Cz-SO at 455 nm are very weak.

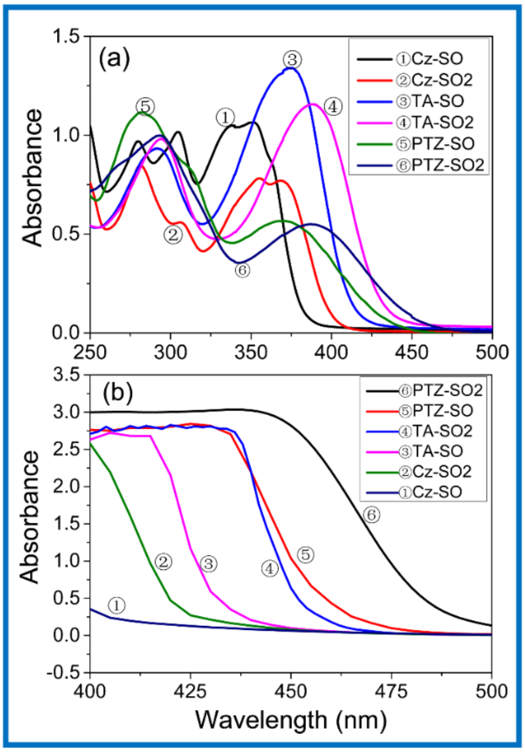

Fig.1 UV-vis absorption spectra of dyes in DCM ((a): M=1×10^{-5}mol/L; (b): M=1×10^{-3}mol/L).

Table 2 Parameters characterizing the reactivity of the dyes: the maximum excitation and emission wavelength (λ_{ex} , λ_{em}) redox potentials (Eox, Ered), the excited state energy (E_{00}), free energy changes (ΔG_{et}),fluorescence quantum yields (Φ_f)

	λ_{ex} (nm)	λ_{em} (nm)	Stoke's shift(nm)	E_{ox} (V)	E_{red} (V)	E_{00} (eV)	ΔG_{et} (eV)	Φ_f
Cz-SO	351	427	76	-1.63	-1.66	3.21	-4.28	0.69
Cz-SO2	369	452	83	-1.50	-1.90	3.07	-4.01	0.75
TA-SO	374	474	100	-1.64	-1.67	2.95	-4.03	0.59
TA-SO2	389	503	114	-1.46	-1.85	2.81	-3.71	0.58
PTZ-SO	370	527	157	-1.60	-1.76	2.72	-3.76	0.29
PTZ-SO2	388	559	171	-1.45	-1.81	2.60	-3.49	0.08
ONI					-0.56			

3.2 One-photon and two-photon fluorescence spectra

The one-photon fluorescence emission spectra of the six dyes in DCM solution are shown in Fig. 2, and the corresponding data are listed in Table 2. From the Table 2 we can get the maximum emissions of Cz-SO, Cz-SO2, TA-SO, TA-SO2, PTZ-SO and PTZ-SO2 were about 427nm, 452nm, 474nm, 503nm, 527nm and 559nm, respectively. The results show that the maximal emission peaks were red-shifted from sulfoxide to sulfone. The fluorescence quantum efficiency of the dyes were tested in DCM solution at a concentration of 1×10^{-6} mol/L, and the relevant data are listed in Table 2. This table clearly shows that the molecules containing carbazole and triphenylamine exhibit higher fluorescence quantum yields than the molecules containing phenothiazine.

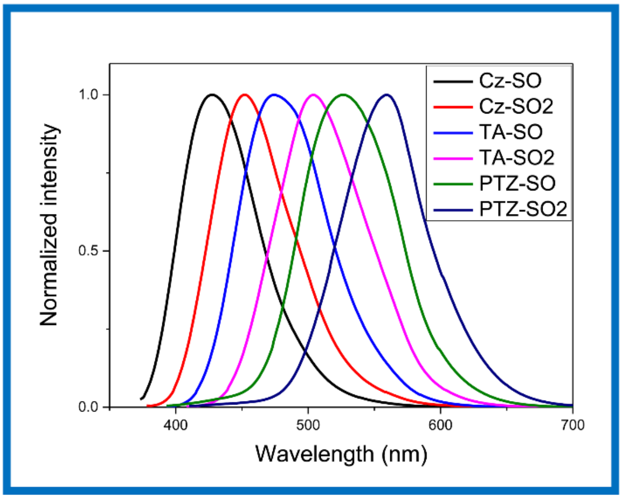

Fig. 2 Normalized fluorescence emission spectra of the dyes in DCM solution ($M=1\times10^{-5}$ mol/L).

TPEF spectra were measured using excitation wavelengths ranging from 700 to 880 nm. The corresponding two-photon excitation spectra of the six dyes in DCM under different excitation laser wavelengths are shown in Fig.S3. The results showed that Cz-SO, Cz-SO2, TA-SO, TA-SO2, PTZ-SO and PTZ-SO2 present the strongest emissions when excited by 730 nm, 720 nm, 730 nm,780 nm, 750 nm and 780 nm laser light.

TPA cross-sections were measured using the two-photon induced fluorescence technique and calculated with Eq. (5). The calculation outcomes of the TPA cross-sections of the dyes under different excitation laser wavelength are shown in Table S1. The corresponding TPA cross-sections of the compounds in DCM at excitation wavelength ranging from 700 nm to 880 nm are shown in Fig.3; this figure reveals that the maximum TPA cross-sections are 220.2 GM for Cz-SO, 221.8 GM for CZ-SO_2, 467.0 GM for TA-SO, 1006.8 GM for TA-SO_2, 336.3 GM for PTZ-SO and 2465.5 GM for PTZ-SO_2, respectively. The results showed that the dyes with sulfone possess higher TPA cross-sections than the same dyes with sulfoxide. This finding suggests that as increases in the with-drawing structure are achieved, two-photon absorption is enhanced. The result proves that the strategy of increasing the ICT effect is an effective approach for enhancing the TPA cross-section of the molecule.

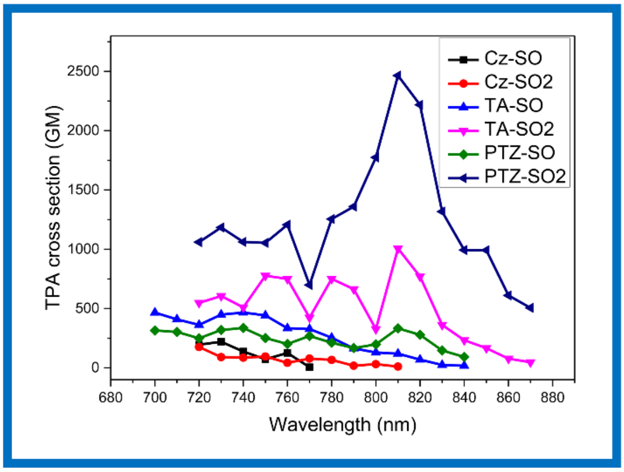

Fig.3 The TPA cross-sections of the dyes in DCM ($M=1\times10^{-4}$mol/L) at different excitation wavelengths.

3.3 Polymerization photoinitiated by the dyes /ONI system

Free radical polymerization of TPGDA in the presence of ONI (1.0 wt%) with dyes (0.1 wt%) was carried out using a laser diode at 405 and 455 nm, respectively. A small amount of NMP was added as the solvent. The double bond conversion rate vs. time curves of the photocurable resin films containing different dyes were obtained, and the results are shown in Fig.4 (a), (b), (d), and Table 3. Cationic

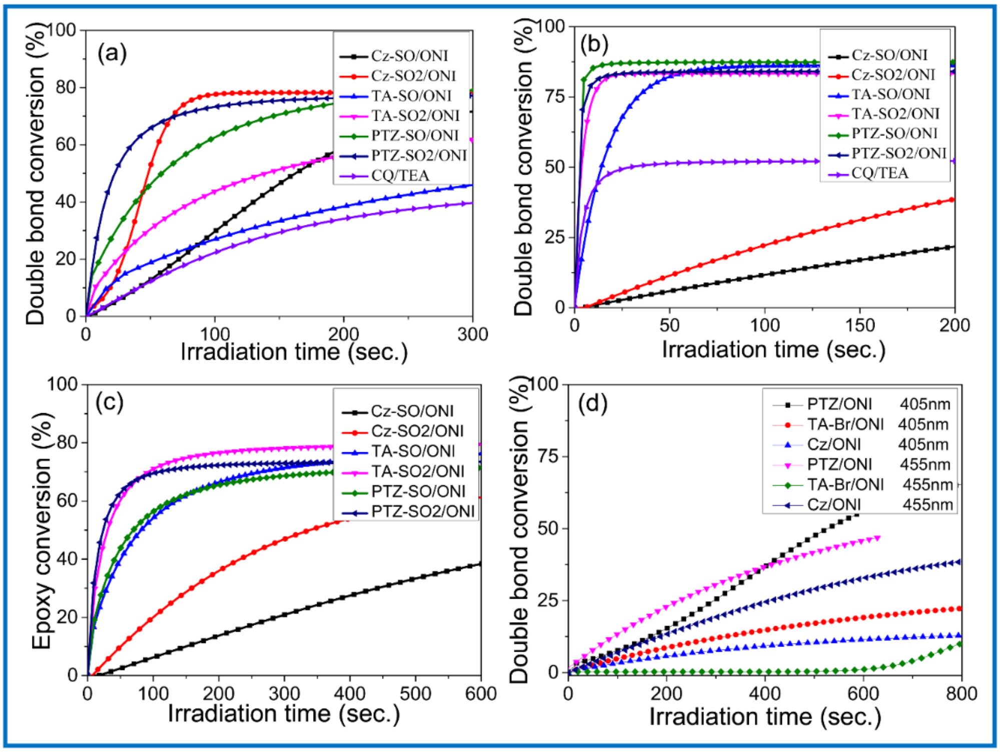

Fig.4 Photopolymerization profiles of TPGDA in a laminate in the presence of dyes/ONI. (a) under the laser diode at 405 nm. (TPGDA:100 wt%; ONI: 1.0 wt%; dyes: 0.1%).(b) under the laser diode at 455 nm (TPGDA:100 wt%; ONI: 1.0 wt%; dyes: 0.1%). (c) under the laser diode at 455nm (E51:100 wt%; ONI: 3.0 wt%; dyes: 0.1%). (d) the comparing experiments TPGDA: 100wt%; ONI : 1.0 wt% ; Cz, TA-Br and PTZ: 0.1%).

Table3 Conversions of TPGDA and E51 in a laminate upon exposure to laser diode sources in the presence of dye-based ONIs. (TPGDA: 100 wt%; ONI: 1.0 wt%; dyes: 0.1wt%. And E51:100wt%; ONI: 3.0wt%; dyes: 0.1wt%).

	TPGDA				E51
	405nm		455nm		455nm
	100s	200s	20s	100s	(final conversion)
Cz-SO/ONI	29%	59%	2%	12%	39%
Cz-SO2/ONI	78%	78%	4%	22%	61%
TA-SO/ONI	27%	38%	61%	86%	73%
TA-SO2/ONI	44%	56%	83%	83%	79%
PTZ-SO/ONI	63%	75%	87%	87%	68%
PTZ-SO2/ONI	73%	76%	84%	84%	73%
Cz/ONI	3%	6%	2%	7%	-----
TA-Br/ONI	5%	9%	0.3%	0.3%	-----
PTZ/ONI	14%	15%	4%	14%	-----
CQ/TEA	22%	34%	48%	52%	-----

polymerization of E51 in the presence of dyes (0.1 wt%) and ONI (3.0 wt%) was carried out under the laser diode at 455 nm. In the cationic photopolymerization system, a small amount of epoxy chloropropane was added as the solvent. The results are shown in Fig.4 (c) and Table 3.

Our experiment reveals that dyes have no photoinitiating ability when used only by themselves under a laser at 405 and 455 nm. For comparison, camphorquinone (CQ)/triethanolamine (TEA), Cz/ONI, TA-Br/ONI, and PTZ/ONI were tested as photoinitiators at the same experimental conditions. The results of the comparison experiments are shown in Fig. 4 (d) and Table 3. The results show that the photoinitiating efficiencies of TPGDA of Cz/ONI, TA-Br/ONI, and PTZ/ONI are very low under the laser diode at 405 and 455 nm, whereas E51 almost had no polymerization.

The photopolymerization experiments reveal that under the laser diode at 405 nm (as shown in Fig.4 (a)), all dyes/ONI photoinitiating systems have higher efficiency than well-known CQ/TEA couple photoinitiating systems. The conversion of comparison systems CQ/TEA is about 40%, and the time they needed to reach the level are above 300 s. The conversions of PTZ-SO/ONI and PTZ-SO2/ONI can reach up to 63% and 73%, respectively, when the irradiation time is

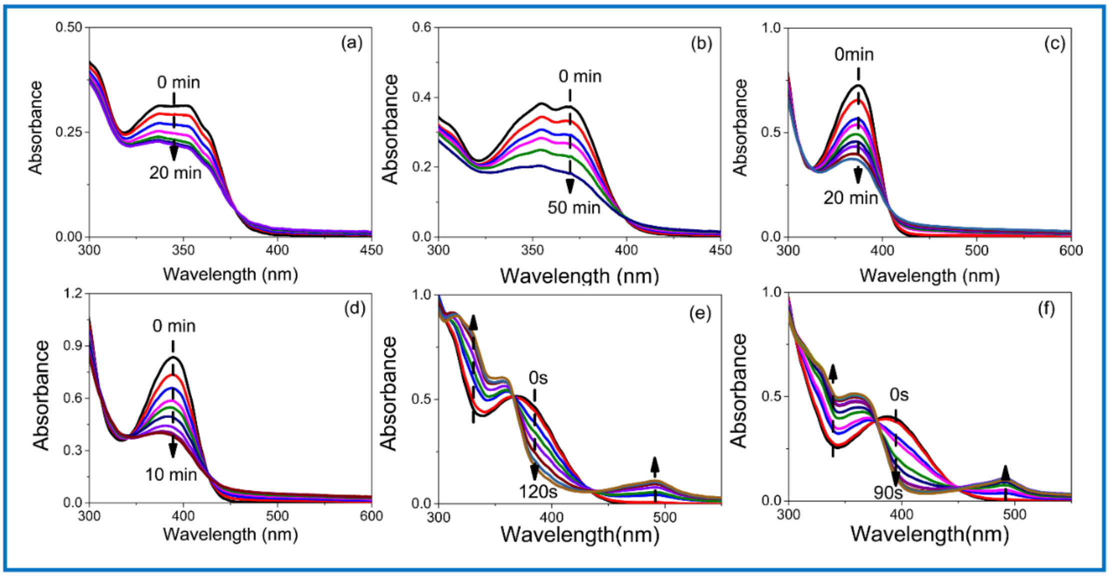

Fig.5. Photolysis of (a) Cz-SO/ONI, (b) Cz-SO2/ONI, (c) TA-SO/ONI, (d)TA-SO2/ONI, (e) PTZ-SO/ONI, (f) PTZ-SO2/ONI, in DCM upon the a laser diode at 455 nm exposure (M_{dye}= 5×10^{-6} mol/L , M_{ONI}=1×10^{-3} mol/L , m_{dye}:m_{ONI}=10:1); UV-vis spectra were recorded at different irradiation times.

100 s. The conversion of Cz-SO/ONI and Cz-SO2/ONI can reach up to 59% and 78%, respectively, when the irradiation time is 200 s. The photoinitiating efficiency order is PTZ-SO2/ONI>PTZ-SO/ONI>Cz-SO2/ONI>Cz-SO/ONI>TA-SO2/ONI>TA-SO/ONI.

Compared with the results of photopolymerizaiton under the laser diode at 405 nm, the results from the photopolymerization profiles of TPGDA under the laser diode at 455 nm (Fig. 4 (b)) show that the conversions of Cz-SO/ONI and CZ-SO2/ONI can only reach up to 21% and 39%, respectively, when the irradiation time is 200 s. However, the final conversions of TA-SO/ONI (Cf=86%) and TA-SO2/ONI (Cf=83%) are much higher than the conventional system CQ/TEA. TA-SO/ONI needs 73 s to reach 86%, whereas TA-SO2/ONI only needs 20 s. The most efficient photopolymerization systems are PTZ-SO/ONI (Cf=87%) and PTZ-SO2/ONI (Cf=84%), which could reach above 84% within 10 s of irradiation. Photoinitiating efficiency order under the laser diode at 455 nm is PTZ-SO2/ONI≈PTZ-SO/ONI>TA-SO2/ONI>TA-SO/ONI>Cz-SO2/ONI>Cz-SO/ONI.

As shown in Fig.4(c), the epoxy conversions of Cz-SO/ONI and Cz-SO2/ONI reached 39% and 61%, respectively, within 600 s of irradiation. The final epoxy conversion of TA-SO2/ONI (Cf=79%) was higher than TA-SO/ONI (Cf=73%). In addition, PTZ-SO2/ONI (Cf=73%) is more efficient than PTZ-SO/ONI (Cf=68%). From these results, sulfones have a much higher efficiency and that triphenylamine and N-ethyl phenothiazine have nearly the same efficiency but much better than N-ethyl carbazole.

The results from photopolymerizaiton are related to the UV–vis absorption of the dyes in DCM (Table 1). Cz-SO and Cz-SO2 have weak absorption at 455 nm. Their molar extinction coefficients are 60 and 80 $M^{-1}cm^{-1}$. TA-SO, TA-SO2, PTZ-SO, and PTZ-SO2 have stronger absorption, with molar extinction coefficients of 2650, 5070, 1580, and 8040 $M^{-1}cm^{-1}$, respectively.

3.4 Photobleaching of the Dye/ONI solution

Experiments of photobleaching of the dye/ONI solution upon laser diode exposure at 455 nm were carried out in open air. To study the dye/ONI interaction, the UV-vis spectra of the dye/ONI solution in DCM were recorded at different irradiation times, as shown in Fig.5. For comparison, the photolysis of dye in DCM was measured, and their UV-vis spectra are all the same at different irradiation times. During the irradiation of dye/ONI in DCM, significant bleaching of all dye/ONI was clearly observed.

Fig.5 (a), (b), (c), and (d) show that during the irradiation of Cz-SO/ONI, Cz-SO2/ONI, TA-SO/ONI, and TA-SO2/ONI in DCM solution, the spectra change dramatically with a decrease in absorption at 345, 370, 374, and 389 nm, respectively. The reason is that Cz-SO, Cz-SO2, TA-SO, and TA-SO2 were consumed under the irradiation of the laser diode at 455 nm, thereby demonstrating that intramolecular charge transfer exists between dye and ONI.

Fig.5 (e) shows that at the same time PTZ-SO is consumed, a new absorbance appears at 492 nm, which increased with irradiation time. As shown in Fig.5 (f), similar appearances were observed. When the absorbance at 389 nm decreased, a new absorbance appeared at 492 nm, which increased with irradiation time. The reason may be that excited dye molecule formed an exciplex with ONI, and this complex was irreversibly decomposed by an electron-transfer mechanism[14,43-48] to form a dye radical cation absorbing at 492 nm plus initiating radicals.

The photobleaching efficiencies of different systems were calculated from the A/A_0 ratio, where A is the absorbance of the assigned wavelength (e.g., Cz-SO: 345 nm) at different irradiation times and A_0 is the absorbance before irradiation. This data is presented in Fig.6. As seen in Fig.6, the photobleaching efficiency trend of different systems is PTZ-SO2/ONI>PTZ-SO/ONI>TA-SO2/ONI>TA-SO/ONI>Cz-SO2/ONI>Cz-SO/ONI. This result is almost the same as the radical polymerization at 455 nm.

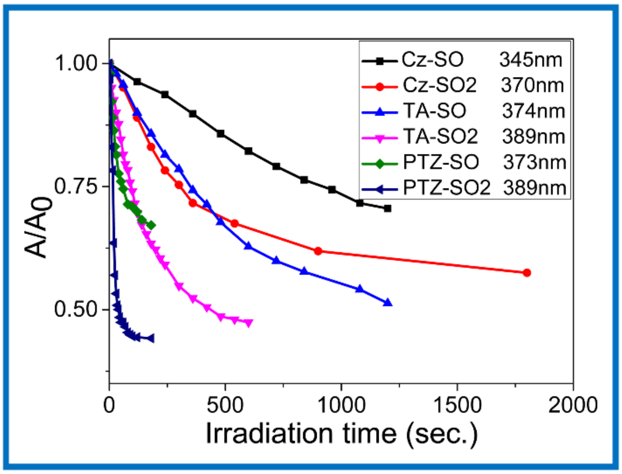

Fig. 6 Photobleaching kinetics of dye/ONI measured under the laser diode at 455nm. (M_{dye}= 5×10^{-6} mol/L, M_{ONI}=1×10^{-3} mol/L , m_{dye}:m_{ONI}=10:1)

3.5 Dye/ONI electron transfer photosensitizing mechanism

The ground state geometry optimizations and the molecular frontier orbitals of Cz-SO2, TA-SO2 and PTZ-SO2 have been shown in Fig.7, Cz-SO, TA-SO and PTZ-SO was shown Fig. S4. The highest occupied molecular orbital (HOMO) of these compounds is almost delocalized over the whole molecule, While the lowest unoccupied molecular orbital (LUMO) levels for all of the compounds are nearly completely localized on the diphenyl-sulfoxide and dipheny-sulfone, respectively. These results indicate that the HOMO–LUMO absorption transition bears an intramolecular charge transfer nature besides π-π^* transition.

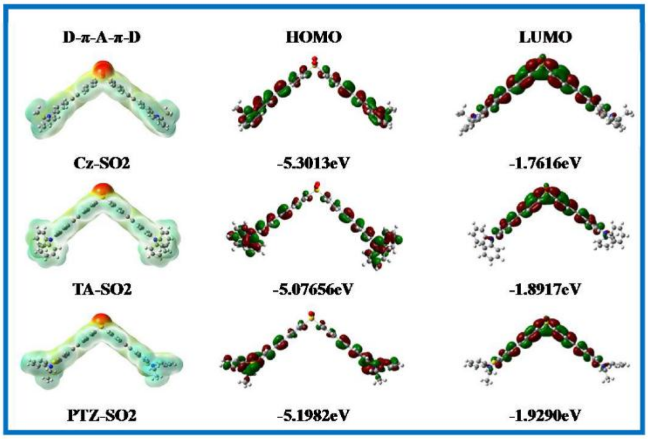

Fig.7 Optimized geometry, highest occupied molecular orbital (HOMO) and lowest unoccupied molecular orbital (LUMO) of CZ-SO2, TA-SO2 and PTZ-SO2 at the B3LYP/6-31G* level.

So far, there have been several mechanisms to explain the photosensitization of onium salts. However, the most efficient and generally applicable process for this class of photoinitiators is electron-transfer photosensitization. As we consider the photoinitiation mechanism of dye/ONI photoinitiation systems, electron transfer is the main process by which these bimolecular systems generate active free radicals to initiate the polymerization of acrylate monomers. Therefore, cyclic voltammograms (CV) and fluorescence spectra of dye were carried out to demonstrate the possibility of an electron transfer process between dye and ONI. The CV curves were shown in Fig.8 (Fig.S5 and Fig.S6), the calculated ΔG_{et} are listed in Table 2.

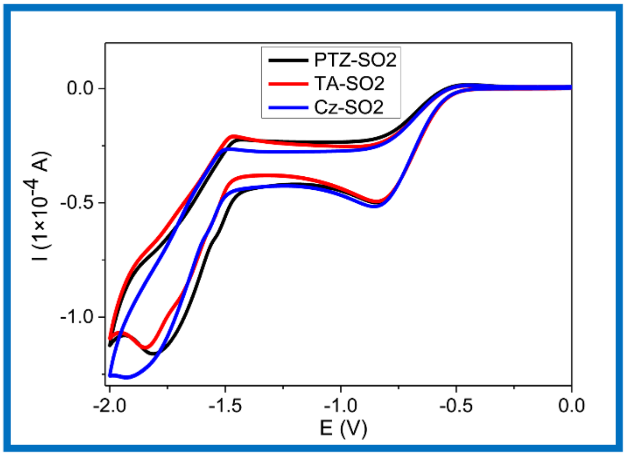

Fig8: Cyclic voltammogram curves of Cz-SO2, TA-SO2 and PTZ-SO2 in DCM (M_{dye}=1.01×10^{-3} mol/L).

Accordingly, the mechanism of the photoinitiating systems involved in the current paper is proposed (Scheme 4). The excited sensitizers (dye*) (1) was produced by the irradiation of light, forming the exciplex, and then oxidated by the ONI leading to dye$^{\bullet+}$ and onium salt radical (C-Ph)$_2$I$^{\bullet}$) (3). The onium salt radical was then cleaved to yield a 4-methyl phenyl radical (C-Ph$^{\bullet}$) (4), neutral molecule C-Ph-I. The monomer can then be polymerized. In addition, Brφnsted acid was generated (7, 8), which can cause epoxy polymerization.[16,20,49] The photosensitizing mechanism can be typically described as follows:

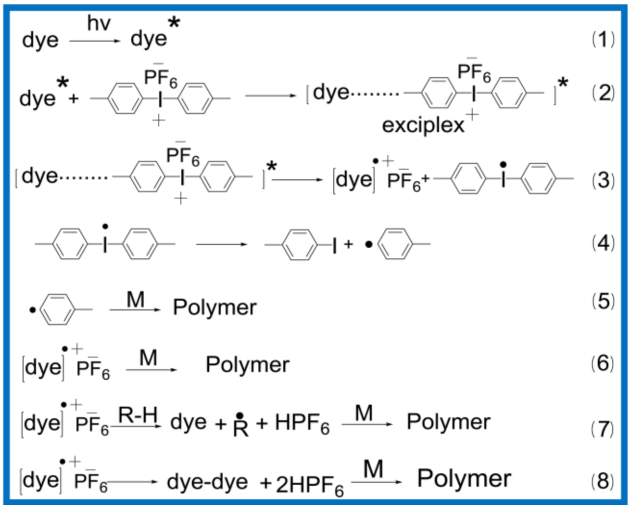

Scheme 4. The mechanism of the photoinitiating systems involved in the current paper.

4 Conclusions

In this work we have synthesized six novel D–π–A–π–D structural photosensitizers, and studied their linear and nonlinear optical properties systemically. The maximum TPA cross-section obtained with femtosecond laser pulses were 220.2 GM for Cz-SO, 221.8 GM for CZ-SO_2, 467.0 GM for TA-SO, 1006.8 GM for TA-SO_2, 336.3 GM for PTZ-SO and 2465.5 GM for PTZ-SO_2, respectively. The results suggest that as increases in the with-drawing structure are achieved, two-photon absorption is significantly enhanced. In addition, their one-photon photopolymerization efficiency in the presence of ONI was studied. The study demonstrates that dye/ONI systems are capable of initiating free radical polymerization of TPGDA. Their photopolymerization efficiency under laser diode at 405 and 455 nm was high. The most efficient photopolymerization systems were PTZ-SO2/ONI and PTZ-SO/ONI, which could reach above 84% within 10 s of irradiation under 455 nm. In addition, DYE/ONI systems could be used in the cationic polymerization of E51. The polymerization efficiency trends of different systems were PTZ-SO2/ONI and PTZ-SO/ONI>TA-SO2/ONI and TA-SO/ONI>Cz-SO2/ONI and Cz-SO/ONI. All the results suggest these dye would have extensive application prospects in two-photon microfabrication and high density optical data storage; and extending the wavelength of the photosensitizers is expected to pave the way for future development of novel photosensitizers.

Acknowledgements

The authors wish to thank for financial support of national natural science foundation of China (Project Grant No. 21176016) and the Fundamental Research Funds for the Central Universities (YS1406). We also thank Beijing University of Chemical Technology CHEMCLOUDCOMPUTING Platform for providing calculating support.

Notes and references

[a]State Key Laboratory of Chemical Resource Engineering, College of Science, Beijing University of Chemical Technology, Beijing 100029, PR China, Tel.: 0086-010-64445350, E-mail: wangtwj2000@163.com

[b]Department of Organic Chemistry, College of Science, Beijing University of Chemical Technology, Beijing 100029, PR China

†Electronic Supplementary Information (ESI) available: [details of any supplementary information available should be included here]. See DOI: 10.1039/b000000x/

References

1. J. P. Fouassier, In Photoinitiation, Photopolymerization and Photocuring: Fundamentals and Applications; Hanser Publishers: Munich,1995.
2. J. V. Crivello, Photoinitiators for Free Radical, Cationic and Anionic Photopolymerization, ed. G. Bradley, New York, 2nd edn, 1998.
3. Photoinitiated Polymerization, ed. K. D. Beled and J. V. Crivello, ACS Symposium series 847, Washington DC, 2003.
4. J. Zhang, M. Frigoli, F. Dumur, P. Xiao, L. Ronchi, B. Graff, F. Morlet-Savary, J. P. Fouassier, D. Gigmes and J. Lalevée, Macromolecules, 2014, 47, 2811-2819.
5. P. Xiao, F. Dumur, B. Graff, F. Morlet-Savary, D. Gigmes, J. P. Fouassier and J. Lalevée, Macromolecules, 2014, 47, 973-978.
6. P. Xiao, F. Dumur, B. Graff, D. Gigmes, J. P. Fouassier and J. Lalevée, Macromolecules, 2014, 47, 601-608.
7. J. Zhang, P. Xiao, F. Morlet-Savary, B. Graff, J. P. Fouassier and J. Lalevee, Polymer Chemistry, 2014, 5, 6019-6026.
8. P. Xiao, F. Dumur, M. Frigoli, M.-A. Tehfe, B. Graff, J. P. Fouassier, D. Gigmes and J. Lalevee, Polymer Chemistry, 2013, 4, 5440-5448.
9. K. Wang, S. Jiang, J. Liu, J. Nie and Q. Yu, Progress in Organic Coatings, 2011, 72, 517-521.
10. G. Temel, B. Enginol, M. Aydin, D. K. Balta and N. Arsu, Journal of Photochemistry and Photobiology A: Chemistry, 2011, 219, 26-31.
11. G. Temel, B. Aydogan, N. Arsu and Y. Yagci, Macromolecules, 2009,42, 6098–6106.
12. S. K. Dogruyol, Z. Dogruyol and N. Arsu, Journal of Polymer Science Part A: Polymer Chemistry, 2011, 49, 4037-4043.
13. V. Mucci and C. Vallo, Journal of Applied Polymer Science, 2012, 123, 418-425.
14. D. Tunc and Y. Yagci, Polymer Chemistry, 2011, 2, 2557-2563.
15. Y. Hua and J. V. Crivello, Journal of Polymer Science Part A: Polymer Chemistry, 2000, 38, 3697-3709.
16. Y. Hua and J. V. Crivello, Macromolecules, 2001, 34, 2488-2494.
17. Z. Gomurashvili, Y. Hua and J. V. Crivello, Macromolecular Chemistry and Physics, 2001, 202, 2133-2141.
18. Z. Gomurashvili and J. V. Crivello, Journal of Polymer Science Part A: Polymer Chemistry, 2001, 39, 1187-1197.
19. Y. Chen, T. Yamamura and K. Igarashi, Journal of Polymer Science Part A: Polymer Chemistry, 2000, 38, 90-100.
20. Z. Gomurashvili and J. V. Crivello, Macromolecules, 2002, 35, 2962-2969.
21. H. Zhou, F. Zhou, S. Tang, P. Wu, Y. Chen, Y. Tu, J. Wu and Y. Tian, Dyes and Pigments, 2012, 92, 633-641.
22. D. Hu, Y. Hu, W. Huang and Q. Zhang, Optics Communications, 2012, 285, 4941-4945.
23. T. Zhao, K. Yu, L. Li, T. Zhang, Z. Guan, N. Gao, P. Yuan, S. Li, S. Q. Yao, Q.-H. Xu and G. Q. Xu, ACS Applied Materials & Interfaces, 2014, 6, 2700-2708.
24. H. M. Kim, B. H. Jeong, J.-Y. Hyon, M. J. An, M. S. Seo, J. H. Hong, K. J. Lee, C. H. Kim, T. Joo, S.-C. Hong and B. R. Cho, Journal of the American Chemical Society, 2008, 130, 4246-4247.
25. C. Zhao, M. Burchardt, T. Brinkhoff, C. Beardsley, M. Simon and G. Wittstock, Langmuir, 2010, 26, 8641-8647.
26. R. Nazir, E. Balčiūnas, D. Buczyńska, F. Bourquard, D. Kowalska, D. Gray, S. Maćkowski, M. Farsari, D.T.Gryko .Macromolecules, 2015, 48, 2466−2472
27. H. Yuan, Y. Zhao and F. Wu, Chemistry of Materials, 2012, 24, 1371-1377.
28. J. Xue, Y. Zhao, F. Wu and D.-C. Fang, The Journal of Physical Chemistry A, 2010, 114, 5171-5179.
29. J. Wu, Y. Zhao, X. Li, M. Shi, F. Wu and X. Fang, New Journal of Chemistry, 2006, 30, 1098-1103.

30. M. Jin, J. Xie, J.-P. Malval, A. Spangenberg, O. Soppera, D.-L. Versace, T. Leclerc, H. Pan, D. Wan, H. Pu, P. Baldeck, O. Poizat and S. Knopf, Journal of Materials Chemistry C, 2014, 2, 7201-7215.
31. J. Ye, Z. Chen, M.-K. Fung, C. Zheng, X. Ou, X. Zhang, Y. Yuan and C.-S. Lee, Chemistry of Materials, 2013, 25, 2630-2637.
32. K. P. Boroujeni, Phosphorus, Sulfur, and Silicon and the Related Elements, 2010, 185, 2085-2091.
33. M. Planells, A. Abate, D. J. Hollman, S. D. Stranks, V. Bharti, J. Gaur, D. Mohanty, S. Chand, H. J. Snaith and N. Robertson, Journal of Materials Chemistry A, 2013, 1, 6949-6960.
34. A. L. Thompson, T.-S. Ahn, K. R. J. Thomas, S. Thayumanavan, T. J. Mart ńez and C. J. Bardeen, Journal of the American Chemical Society, 2005, 127, 16348-16349.
35. J. W. Stansbury and S. H. Dickens, Dental Materials, 2001, 17, 71-79.
36. B. Jiang and Y. D. Huang, Composites Part A: Applied Science and Manufacturing, 2008, 39, 712-717.
37. B. Jędrzejewska, J. Jeziórska and J. Pączkowski. Journal of Photochemistry and Photobiology A: Chemistry, 2008, 195, 105-115.
38. D. Rehm and A. Weller, Israel Journal of Chemistry, 1970, 8, 259-271.
39. J. Sokołowska, R. Podsiadły and J. Stoczkiewicz, Dyes and Pigments, 2008, 77, 510-514.
40. K. Rurack. Fluorescence quantum yields: methods of determination and standards. Springer Ser.Fluoresc. 2008, 5, 101-145.
41. D. Li, Q. Zhang, X. Sun, N. Shao, R. Li, S. Li, H. Zhou, J. Wu and Y. Tian, Dyes and Pigments, 2014, 102, 79-87.
42. C. Xu and W. W. Webb, Journal of the Optical Society of America B, 1996, 13, 481-491.
43. J. V. Crivello, Journal of Polymer Science Part A: Polymer Chemistry, 1999, 37, 4241-4254.
44. E. W. Nelson, T. P. Carter and A. B. Scranton, Journal of Polymer Science Part A: Polymer Chemistry, 1995, 33, 247-256.
45. J. V. Crivello, J. M, F. Jiang, H. Hua, J. Ahn and R. Acosta Ortiz, Macromol Symp, 2004, 215, 165-177.
46. Y. Bi and D. C. Neckers, Journal of Photochemistry and Photobiology A: Chemistry, 1993, 74, 221-230.
47. S. Beyazit, B. Aydogan, I. Osken, T. Ozturk and Y. Yagci, Polymer Chemistry, 2011, 2, 1185-1189.
48. R. Podsiadły, A. Maruszewska, R. Michalski, A. Marcinek and J. Kolińska, Dyes and Pigments, 2012, 95, 252-259.
49. M.-A. Tehfe, F. Dumur, B. Graff, F. Morlet-Savary, D. Gigmes, J.-P. Fouassier and J. Lalevee, Polymer Chemistry, 2013, 4, 3866-3875.